A High Sensitivity of Vital Signs Detector using Fiber Optic-based Fabry-Perot Interferometer

Saroj Pullteap† and **Piyawat Samartkit**, Non-members

ABSTRACT

In this paper, development of a high sensitivity vital sign detector based on the fiber optic-based Fabry-Perot interferometer (FFPI) has been proposed. Two interesting parameters, heart rate (HR), and blood pressure (BP), are measured as the vital sign parameters for investigating the performance of the FFPI. Particularly, the proposed sensor is exploited to detect human arterial pulse for indicating the number of interference signals (fringes). A fringe counting technique is, consequently, applied in association with the deflection of material technique to demodulate the observed number of fringes into HR and BP. Additionally, the reflective thin film with reflectance of approximately 55% is utilized for attaching to the human wrist during the measurement. Furthermore, a digital sphygmomanometer is employed as a reference sensor. After 20 times of repetitions on the same human subject, the FFPI could indicate the systolic and diastolic BP, as well as HR, with average error of 0.94%, 1.64%, and 1.01%, respectively. Moreover, the sensitivity of 1.913 mmHg has been exploited by using the fiber optic sensor, while the reference is reported to be 40 mmHg. This could, thus, verify that the FFPI sensor is a very high sensitivity instrument for applying to the vital sign measurement.

Keywords: Fabry-Perot Interferometer, Fringe Counting Technique, Deflection of Material Technique, Vital Signs, Biomedical Engineering Applications

1. INTRODUCTION

Vital cardiovascular signs are important health indicators. Specifically, both the heart rate (HR) and blood pressure (BP) are, basically, always considered in the medical diagnosis, for which these values reflect the health or disease of an individual [1–2]. As such, distribution of commercial vital cardiovascular signs equipment is emphasized, since this enables anyone to easily diagnose their cardiovascular health in everyday life, and allows at-home BP control to prevent cardiovascular disease, such as hypertension [3–4]. However, the commercial non-invasive digital sphygmomanometers tend to be less precise than the medical diagnostic standard, or are vulnerable to strong electromagnetic interference and electrical noise, which cause them to be less reliable [5–7]. In this aspect, the fiber optic sensors (FOS) are, therefore, introduced with several advantages, i.e. high sensitivity & precision, electromagnetic immunity [8–9]. Consequently, there are many medical instruments that have, recently, adopted FOS to improve their performance [10]. For example, Jia *et al.* [11] present a radial arterial pulse detector using FOS for highly sensitive acquisition. Additionally, Leitão *et al.* [12–13] designed fiber optic sensor-based instruments to measure the central arterial pulse, which is, generally, difficult to detect due to low BP. Meanwhile, Nedoma *et al.* [14] demonstrated the vital signs FOS applicability during the magnetic resonance imaging (MRI) procedure. As such, it could be concluded that FOS provides improved performance to medical measurement instrumentations.

In this work, development of a highly sensitive vital cardiovascular signs detector based on the fiber optic-based Fabry-Perot interferometer (FFPI) has been proposed. Particularly, the interesting parameters of HR, systolic blood pressure (SBP), and also diastolic blood pressure (DBP) are measured via the FFPI sensing principles. Furthermore, signal demodulation has been completed by applying the deflection of material and fringe counting techniques [8–9]. Moreover, three reflective materials are tested to determine the optimum material for the fiber sensor measurement. To verify the FFPI performance and its sensitivity, a commercial digital sphygmomanometer is, consequently, utilized as a reference sensor, with the results discussed to motivate FFPI development in the future.

Manuscript received on September 26, 2019 ; revised on November 22, 2019 ; accepted on November 28, 2019. This paper was recommended by Associate Editor Chanon Warisarn.

The authors are with the Department of Mechanical Engineering, Faculty of Engineering and Industrial Technology, Silpakorn University (Sanam Chandra Palace), Nakhon Pathom, Thailand.

†Corresponding author. E-mail: saroj@su.ac.th

Digital Object Identifier 10.37936/ecti-eec.2020182.218271

2. RELATED THEORIES

2.1 Principles of FFPI sensor

Fiber optic-based Fabry-Perot interferometer is one of the fiber optic interferometers that is often utilized for precision measurement applications. Particularly, it operates when a monochromatic light is propagated through a fiber coupler, before propagating to the sensing arm. Approximately 4% of the propagated light beam is, then, reflected back at the fiber cave-end as the "*reference signal*", whereas the rest is transmitted to the target. Consequently, the 96% light beam is to be reflected back to the fiber as the "*sensing signal*". The interference signal is, ultimately, generated when the two light beams are superpositioned, with the intensity of the modulated signal (I) depicted by [8–9]:

$$I = I_R + I_S + 2\sqrt{I_R I_S}\cos\Delta\phi \tag{1}$$

where I_R is the reference signal intensity, I_S indicates the sensing signal intensity, and $\Delta\phi$ corresponds to the optical path difference between the reference and sensing signal. Coincidentally, $\Delta\phi$ is related to the displacement length from the fiber cave-end to the sensing target (Δd), along with the number of fringes (N_f). These could be mathematically described as [8–9], [15]:

$$\Delta\phi = \frac{4\pi Nn}{\lambda}\Delta d = 2\pi N_f \tag{2}$$

where N indicates the total number of reflections, n depicts the refractive index, and λ is the light source wavelength. Generally, the configuration of the FFPI could be illustrated in Fig. 1.

In this regard, FFPI-based measuring instruments are commonly designed to detect the displacement shift of the target parameters. In this case, the displacement is, however, caused by the distension of the target artery as a consequence of the heart pulse.

2.2 Application of FFPI for HR and BP measurements

To sense the vital signs of HR and BP, the deflection of material theory is proposed. In this case, the reflective thin film is considered as the target material. When there is any arterial pulse at the sensing target, the film would be deflected, and the blood pressure of the pulse (P) could be determined by [16–17]:

$$\Delta d = \frac{3Pr_0^4\left(1-\nu^2\right)}{16Eh^3} \tag{3}$$

where r_0 is the deflection radius, ν depicts the Poisson's ratio, E indicates Young's modulus, and h defines the thickness of the film. These variables could graphically be described in Fig. 2.

The HR of the subject could be detected by observing the peak-to-peak signal during the sensing duration. The BP, however, is measured in correspondence with the inflatable cuff. Conventionally, the blood flow is first stopped due to the pressure of the inflated cuff. The cuff is, continuously, deflated until the first heart pulse is detected, of which the pressure corresponds to the SBP. Consequently, the pressure is released gradually, and the last arterial pulse to be sensed denotes the DBP. In this manner, the fiber sensor could determine both the SBP and DBP values in the measurement by using the fringe counting technique shown in Eq. (2) in association with Eq. (3).

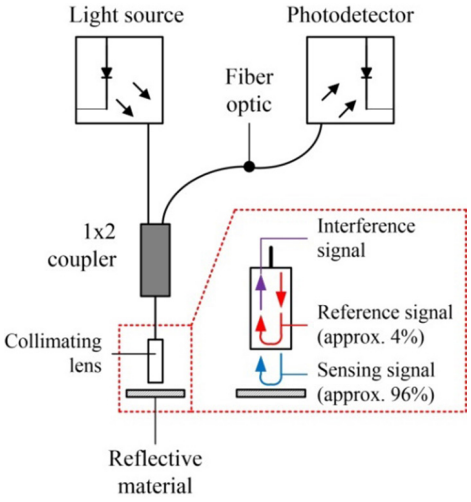

Fig.1: *Basic of FFPI configuration.*

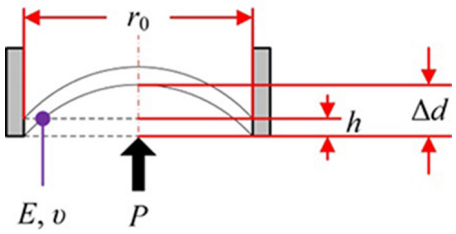

Fig.2: *Concept of deflection of material technique.*

3. EXPERIMENTAL SETUP

In this work, FFPI has been utilized for measuring the HR and BP in a human subject. However, the emphasis is to be given for selecting the reflective material, as implied by Eq. (3) that the material characteristics could affect the demodulation of the light beam signal. Furthermore, experimental setup on a human subject tends to be important, as poor execution might lead to measurement error. As such, this section intends to describe its contents in 3 main parts; the FFPI system configuration, reflective material verification, and human subject examination.

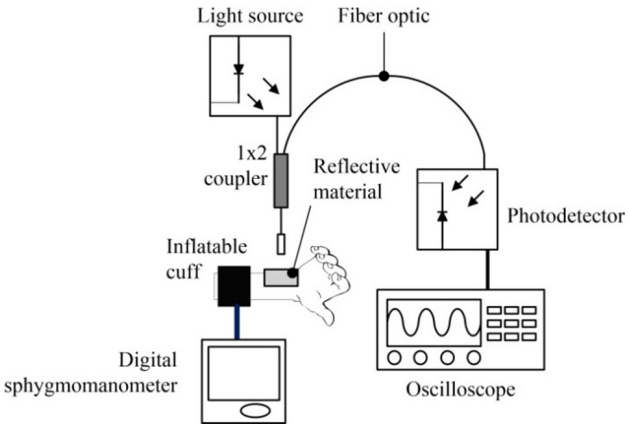

Fig.3: *FFPI system configuration for HR and BP signals acquisition.*

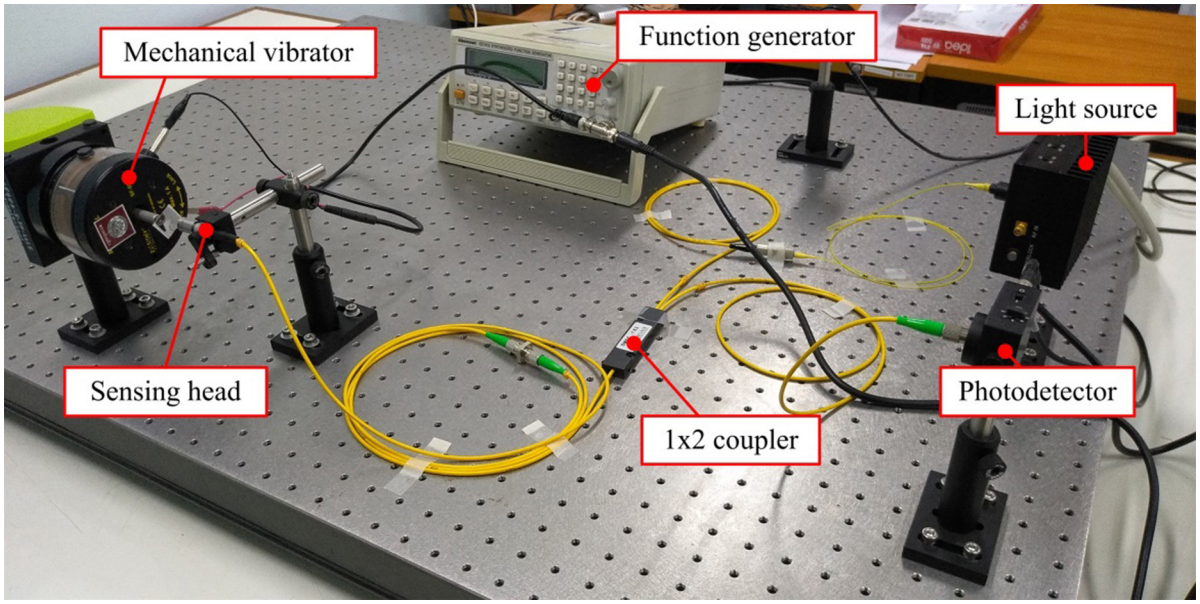

Fig.4: *Configuration of FFPI system for reflective material verification.*

3.1 FFPI system configuration

To properly measure the arterial pulse, an indicator of both HR and BP, the FFPI measurement system is setup. In particular, the configuration of the fiber optic sensor could be illustrated by Fig. 3.

According to Fig. 3, the monochromatic light source from the laser diode source is generating a light beam of 1,310 nm wavelength that is injected into the single-mode fiber pigtail cord. Furthermore, this beam is, then, propagated through a 1×2 fiber coupler to the sensing arm, where the sensing beam is guided outside to the target before being reflected back. Ultimately, the interference signal is acquired by a photodetector, and its characteristic waveform is analyzed via a digital oscilloscope. However, a reflective material is required for reflecting the sensing light beam. Therefore, it is crucial to verify the optimum material to be applied for the fiber interferometer system.

3.2 Reflective materials verification

As mentioned in the previous part, reflective material is crucial for the experiment. Consequently, the FFPI system for reflective material verification is used. Its configuration is illustrated in Fig. 4.

To clarify, the system applies the signal generator in conjunction with the mechanical vibrator to simulate the arterial pulse of a patient. In this case, the excitation frequency is 500 mHz, while the excitation amplitude is 200 mV. The reflective material would, consequently, be placed onto the actuating arm of the vibrator before the verification starts. In this regard, the three materials to be verified are the retro-reflector, plastic mirror, and reflective thin film, and the main objective of this experiment is to determine the reflectance of the material, as high reflectance often indicates better sensitivity. Moreover, it is suggested that the material should be compatible for attaching to human

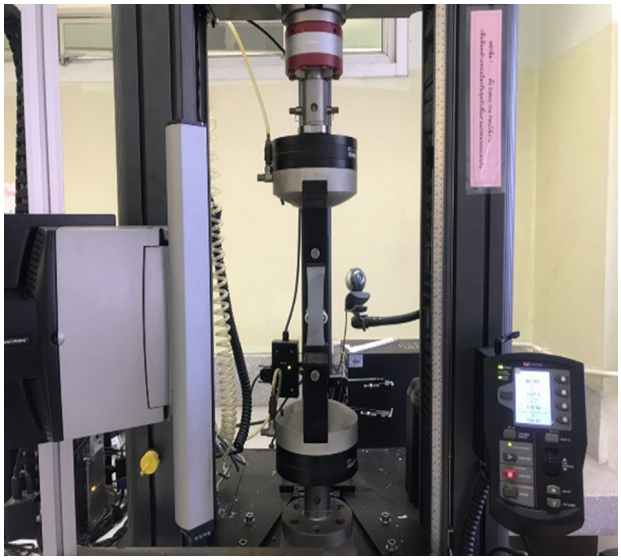

Fig.5: *Tensile testing machine (INSTRON model 5969) for optimum material validation.*

skin, specifically to allow pulse response from the radial artery. Ultimately, the optimum material is selected, before its essential properties of Poisson's ratio, Young's modulus, deflection radius, and thickness, are validated using *INSTRON* universal tensile testing machine *model 5969* shown in Fig. 5.

To further explain the validation process, the Young's modulus would be defined by analyzing the stress-strain curve of the reflective material. The Poisson's ratio, however, would be calculated by considering the lateral (ε_x) and axial strain (ε_y) of the selected reflective material according to the following:

$$\nu = \frac{\varepsilon_x}{\varepsilon_y} = \frac{(\Delta x/x_0)}{(\Delta y/y_0)} \tag{4}$$

where Δx and Δy are the lateral and axial length change, while x_0 and y_0 correspond to the original lateral and axial length, respectively. In this case, Δx and Δy are to be defined by measuring the length change after the sample material is extended by the tensile testing machine.

3.3 Human subject examination

To acquire the HR and BP from the human subject as accurately as possible, there is a necessary setup on the subject's arm of the volunteer, which could thus be demonstrated by Fig. 6.

From Fig. 6, the target is the radial artery on the wrist of the human subject, with the selected material attached to reflect the sensing light beam. As the blood flows through the target area, the deflection of the material would, thus, correspond to the HR and BP values. In addition, the forearm of the subject is strapped, while resting on a supporting platform. This is done to minimize the movement

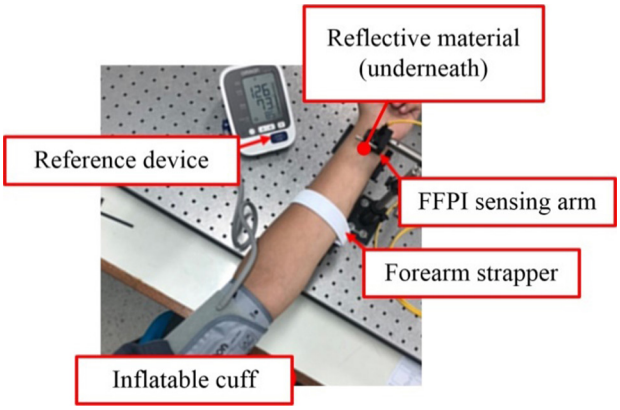

Fig.6: *Experimental setup for human subject examination using FFPI sensor.*

of the forearm, and also reduce as much extraneous vibration from the body as possible. In addition, the inflatable cuff is applied to the upper arm. Consequently, the inflatable cuff of the *Omron HEM 7130* digital sphygmomanometer is used by turning on the device. Therefore, the measurements of HR and BP are simultaneously done by both the proposed FFPI and the reference device.

In this work, the HR and BP measurements are tested on a healthy male subject, who is 22 years old, weighs 64 kg, and is 167 cm tall. Furthermore, the validation is measured in 20 times in repetitions. Finally, the results from the measurement using the FFPI are compared with the reference device to investigate the performance of the proposed sensor.

4. EXPERIMENTAL RESULTS

Initially, the presented materials are verified for determining the optimum object for reflecting the sensing light beam. After using the mechanical vibrator as the pulse simulator, the obtained interference signals of the retro-reflector, plastic mirror, and also reflective thin film are shown in Figs. 7(a)–(c), respectively.

From this experiment, it is found that the retro-reflector has the least reflectance of approximately 20%. Regardless, both the plastic mirror and reflective thin film are suggested to be practical materials, with the reflectance of around 50–55%. However, the plastic mirror tends not to be the optimum material, as it is stiff and unbendable, which obstructed the demodulation technique. Therefore, the reflective thin film is selected for utilization in the FFPI system for measuring the HR and BP.

For the parameters validation, five reflective thin film samples, each having 50 mm in length, 50 mm in width, and 0.55 mm in thickness, were validated. The tensile testing results show the stress-strain curve of the reflective thin film, which are illustrated by Fig. 8.

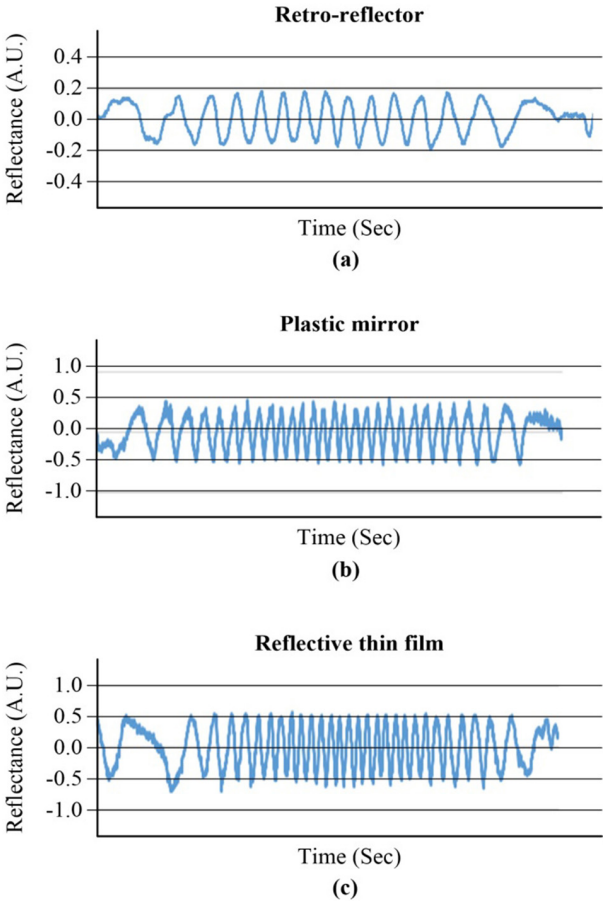

Fig.7: *Output interference signals from material verification: (a) retro-reflector, (b) plastic mirror, and (c) reflective thin film.*

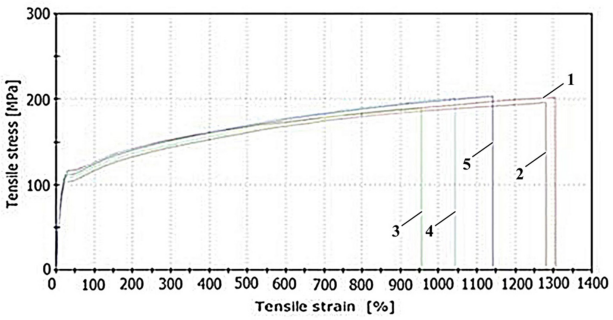

Fig.8: *Stress-strain curve of the validated reflective thin film from tensile testing machine.*

As such, the Young's modulus of the samples are determined by the tensile testing machine, and results are summarized in Table 1.

In addition, the tensile testing machine is utilized to stretch the five reflective thin film samples, with results shown in Fig. 9.

To further explain the details of the mentioned figure, the samples of the reflective thin film are stretched from their original width and length (x_0 and y_0, respectively). After the stretching process,

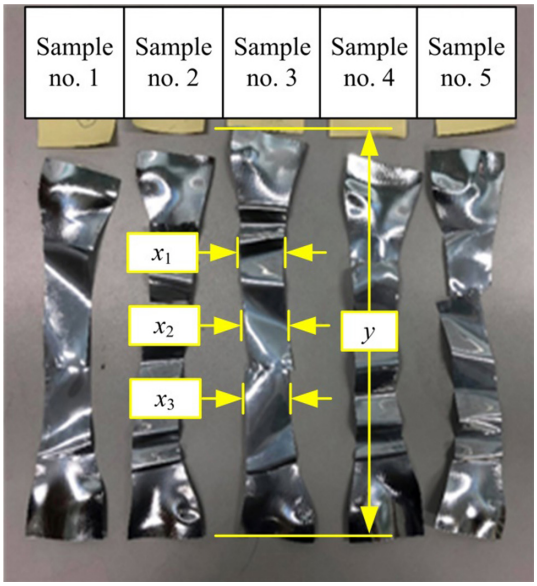

Fig.9: *Material stretching results for Poisson's ratio definition.*

Table 1: *Results of Young's modulus validation.*

Sample no.	Young's modulus (MPa)
1	20,946.37
2	21,964.44
3	21,477.73
4	22,771.34
5	22,174.22
Mean	**21,866.82**

Table 2: *Parameters for Poisson's ratio calculation.*

No.	Δx_1 (cm)	Δx_2 (cm)	Δx_3 (cm)	$\Delta \bar{x}$ (cm)	Δy (cm)
1	2.10	2.15	2.20	2.15	17.20
2	2.30	2.35	2.40	2.35	17.50
3	2.25	2.20	2.25	2.23	19.50
4	2.10	2.20	2.00	2.10	17.30
5	2.35	2.35	2.30	2.33	18.00
Mean				**2.23**	**17.90**

the tested samples are, then, measured for their new sizes. Specifically, the extended length (y) causes the overall width of the material to be shortened, of which three lateral sections, i.e. x_1, x_2, and x_3, are determined to approximate the mean width value. Table 2 summarizes the parameter changes from the material stretching results.

Once the mean values from the mentioned table are calculated by Eq. (4), it is found that the Poisson's ratio of the reflective thin film is 0.125. During the validation, it is also observed that the deflection radius of the film is 1.5 cm. As such, the parameters which would be utilized for the deflection of material theory are presented in Table 3.

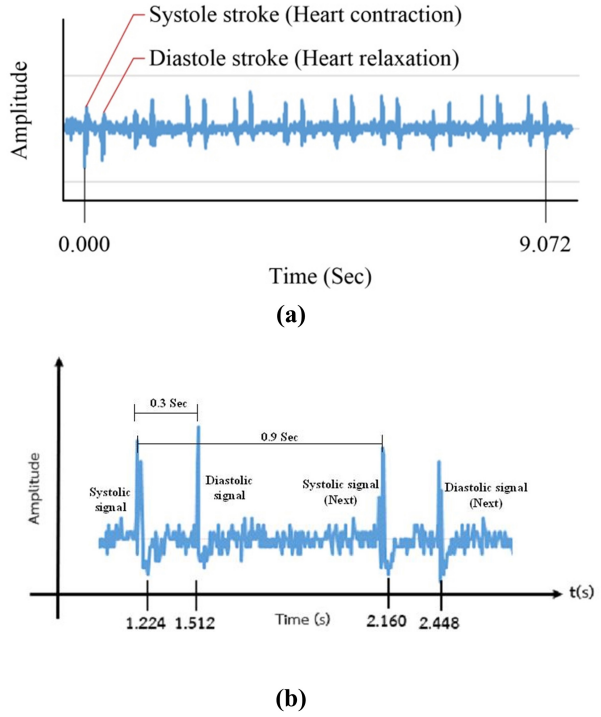

Fig.10: *Interference signal during HR measurement; (a) one complete period of measurement and (b) stroke period.*

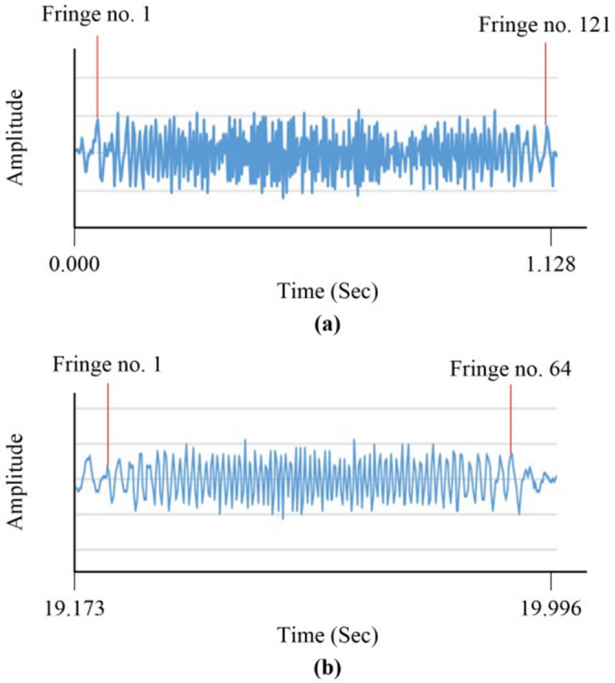

Fig.11: *Interference signal measured by FFPI during BP measurement; (a) SBP period and (b) DBP period.*

Table 3: *Essential properties of reflective thin film for deflection of material theory.*

Parameters	Values
Poisson's ratio (ν)	0.125
Young's modulus (E)	21866.820 MPa
Deflection radius (r_0)	0.015 m
Thickness (h)	0.550 mm

As mentioned in Section 3.3, the FFPI system is utilized to measure the HR and BP of a human subject. The reflective thin film is pasted onto the wrist of the subject as the sensing light beam reflector. Initially, the HR is acquired by observing the peak-to-peak signal for a period of time, as seen in Fig. 10(a).

As mentioned in Fig. 10(a), a single heart pulse has two interference signal peaks. This is further described to be the consequences of the systole and diastole strokes, which correlates to the SBP and DBP, respectively [18].

In addition, further observation, shown by Fig. 10(b), indicates that the systole stroke happens before the diastole stroke by approximately 0.3 s, whereas the next systole stroke occurs 0.9 s after the last one. By scaling the duration of the measurement via a mathematical approach, the HR is demodulated into 66.138 beats per minute (bpm). Additionally, the SBP and DBP are obtained through the inflatable cuff, with results illustrated in Figs. 11(a) and (b), respectively. In this regard, the number of fringes (N_f) during the systole and diastole period is applied in Eq. (2) to define the displacement length (Δd). Consequently, the Eq. (3) could calculate either the SBP or DBP of the human subject. From this figure, however, the calculations indicate the SBP and DBP of 115.729 mmHg, and 61.212 mmHg respectively.

To verify the performance of the proposed FFPI, its measurement results are to be compared with the *Omron HEM 7130*, which is used as a reference sensor. After 20 times of repetitions, the experimental results of the HR, SBP, and DBP are illustrated in Figs. 12(a)–(c), respectively.

The experimental results from Table 4 demonstrated that the reference sensor only displayed measurement values in integer numbers, while the FFPI could indicate the values in decimal forms. This suggests that the FFPI could report more precise measurement results. From the results in Fig. 12, we could summarize that the FFPI has the ability to measure the HR, SBP, and DBP of the human subject, with values approximating to the reference device. Further analysis has found that the SBP measured by the FFPI has an average error of 0.94%, whereas the average error in the DBP and HR measurements are 1.64% and 1.01%, respectively. Furthermore, the measurement errors from the FFPI are indicated in the range from 0.91% to 4.82%, verifying that the fiber optic sensor could be utilized as the HR and BP measuring instrument.

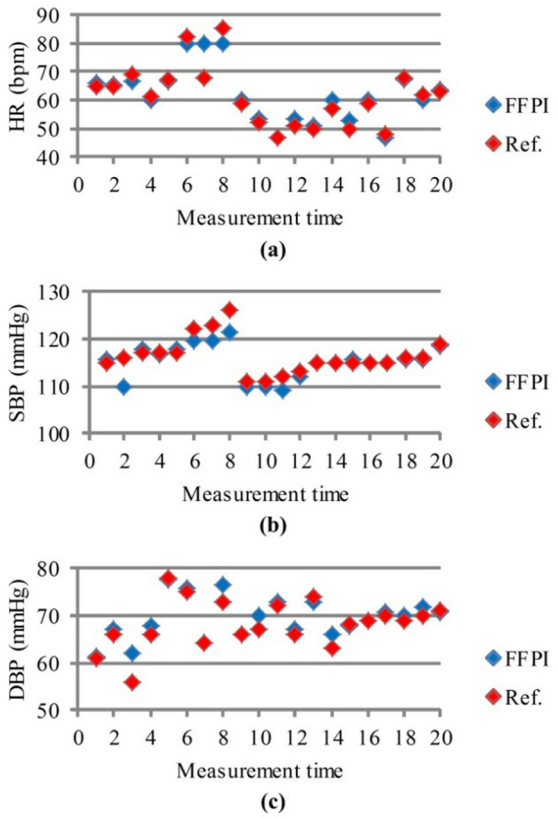

Fig.12: *Measurement results of FFPI and reference device: (a) HR, (b) SBP, and (c) DBP.*

Although the digital reference sphygmomanometer is commercially acceptable, it could be noted from Table 4 that the FFPI is capable of indicating more precise vital signs parameters in terms of significant numbers, due to its high sensitivity. Nevertheless, additional BP simulation using the mechanical vibrator is conducted to validate the BP sensitivity of the proposed FFPI. In this experiment, we generate the vibration frequency of 1 Hz and also adjust the amplitude to be a few millivolts. The experimental result could, however, be illustrated in Fig. 13. It shows that the FFPI has the capability to detect 2 fringes. This translates to a minimum BP reading of approximately 1.913 mmHg, while the reference sensor could not be measured, due to the limitation of the reference equipment. However, we could, preliminary, summarize that the fiber optic sensor has a sensitivity of approximately 1.913 mmHg, while the reference sensor is reported at 40 mmHg (from the manual document).

5. CONCLUSION

In this work, the development of a highly sensitive vital cardiovascular signs detector using the fiber optic-based Fabry-Perot interferometer (FFPI) has been proposed. Specifically, the target parameters are the heart rate (HR), systolic blood pressure (SBP), and diastolic blood pressure (DBP), which could be acquired through the deflection of material, and fringe counting technique. Three reflective materials; the retro-reflector, plastic mirror, and reflective thin film, are tested to select the optimum material for development. In this case, the reflective thin film is chosen, due to its practical reflectance of 55% and its deformability for the demodulation technique. Consequently, a 22 years old healthy male, who weighs 64 kg and is 167 cm tall, is examined for 20 times of measurement repetitions for the human subject examination. Additionally,

Table 4: *Parameters for Poisson's ratio calculation.*

Test no.	SBP (mmHg)		DBP mmHg		HR (bpm)	
	FFPI	Ref.	FFPI	Ref.	FFPI	Ref.
1	115.729	115	61.212	61	66.138	65
2	109.988	116	66.951	66	65.200	65
3	117.639	117	62.167	56	66.700	69
4	116.683	117	67.907	66	60.200	61
5	117.639	117	77.471	78	66.700	67
6	119.552	122	75.559	75	80.000	82
7	119.552	123	64.081	64	80.080	68
8	121.465	126	76.515	73	80.000	85
9	109.988	111	65.994	66	60.27	59
10	109.988	111	69.818	67	53.217	52
11	109.032	112	72.689	72	46.79	47
12	111.901	113	66.950	66	53.571	51
13	114.772	115	72.689	74	50.977	50
14	114.772	115	65.994	63	59.840	57
15	115.728	115	67.907	68	53.000	50
16	114.772	115	68.863	69	59.868	59
17	114.772	115	70.776	70	46.710	48
18	115.728	116	69.819	69	67.347	68
19	115.728	116	71.732	70	60.201	62
20	118.598	119	70.776	71	63.627	63
Mean	**115.202**	**116.3**	**69.294**	**68.2**	**62.022**	**61.4**

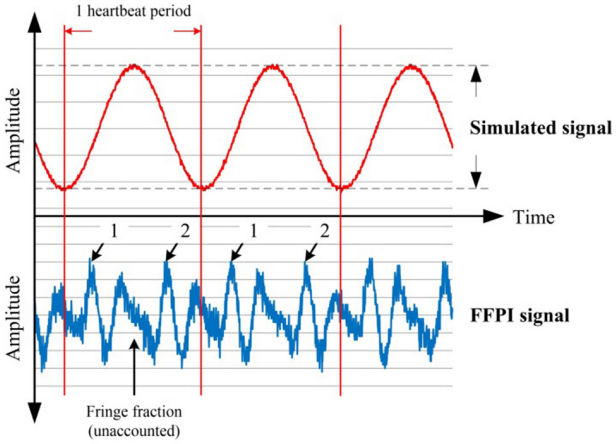

Fig.13: *FFPI interference signal verification in BP simulation.*

the *Omron HEM 7130* digital sphygmomanometer is utilized as the reference device to validate the FFPI performance. The experimental results show that the FFPI could measure the HR, SBP, and DBP, with average errors of 1.01%, 0.94%, and 1.60%, respectively. Furthermore, the proposed sensor has the measurement errors ranging from 0.91% to 4.82%. Nevertheless, it could be suggested that the FFPI is more precise than the commercial sphygmomanometer. Moreover, it is more sensitive to detect the slight arterial pulses with a sensitivity of 1.913 mmHg. This could lead to the prediction of systole and diastole periods in the human subject, which benefits the cardiovascular health monitoring. Likewise, the FFPI is immune to electromagnetic and electrical noise during the measurement, allowing the examination to be done in strong electromagnetic environment, namely the magnetic resonance imaging (MRI) machine. Therefore, it is concluded that the proposed FFPI could be developed into a precise, highly sensitive, and reliable vital cardiovascular signs detector, with more capability in measurement than conventional sphygmomanometers. The main limitation of this sensor is the examination preparation. To clarify, the process tends to require the human subject to position his/her posture correctly before the measurement. This might lead to patient discomfort and difficulty in each examination. Nonetheless, non-invasive commercial instruments often have the drawbacks of either imprecise measurement or being vulnerable to electrical noise and electromagnetic interference, which are irrelevant to fiber optic-based instruments. In this aspect, it is recommended that the fiber optic-based configuration should consider easier human posture positioning and simpler measurement setup for more flexible utilization of the sensor in commercial use. In future work, development of a cuffless non-invasive FFPI for HR and BP measurements would be encouraged, with emphasis on designing a flexible, yet practical, fiber optic-based medical measuring instrument.

References

[1] D. Ettehad *et al.*, "Blood pressure lowering for prevention of cardiovascular disease and death: a systematic review and meta-analysis," *The Lancet*, vol. 387, no. 10022, pp. 957–967, 2016.

[2] M. Volpe, G. Gallo, and G. Tocci, "Novel blood pressure targets in patients with high-normal levels and grade 1 hypertension: Room for monotherapy," *International Journal of Cardiology*, vol. 291, pp. 105–111, 2019.

[3] R. Mukkamala *et al.*, "Toward Ubiquitous Blood Pressure Monitoring via Pulse Transit Time: Theory and Practice," *IEEE Transactions on Biomedical Engineering*, vol. 62, no. 8, pp. 1879–1901, 2015.

[4] K. C. Harris *et al.*, "Hypertension Canada's 2016 Canadian Hypertension Education Program Guidelines for Blood Pressure Measurement, Diagnosis, and Assessment of Risk of Pediatric Hypertension," *Canadian Journal of Cardiology*, vol. 32, no. 5, pp. 589–597, 2016.

[5] A. S. Meidert and B. Saugel, "Techniques for Non-Invasive Monitoring of Arterial Blood Pressure," *Frontiers in Medicine*, vol. 4, no. 231, pp. 1–6, 2018.

[6] J. E. Sharman *et al.*, "Validation of non-invasive central blood pressure devices: ARTERY Society task force consensus statement on protocol standardization," *European Heart Journal*, vol. 38, no. 37, pp. 2805–2812, 2017.

[7] R. Wadhwani, N. Siddiqui, and B. Sharma, "Assessment of accuracy of mercury sphygmo-manometer and automated oscillometric device of blood pressure measurement in population of normal individuals," *Asian Journal of Medical Sciences*, vol. 9, no. 5, pp. 17–24, 2018.

[8] S. Pullteap, "Development of an optical fiber-based interferometer for strain measurements in non-destructive application," *Electrical Engineering*, vol. 99, no. 1, pp. 379–386, 2017.

[9] S. Pullteap and H. C. Seat, "An extrinsic fiber Fabry-Perot interferometer for dynamic displacement measurement," *Photonic Sens.*, vol. 5, no. 1, pp. 50–59, 2015.

[10] M. Fajkus *et al.*, "A Non-Invasive Multichannel Hybrid Fiber-Optic Sensor System for Vital Sign Monitoring," *Sensors*, vol. 17, no. 1, p. 111, 2017.

[11] D. Jia *et al.*, "A Fiber Bragg Grating Sensor for Radial Artery Pulse Waveform Measurement," *IEEE Transactions on Biomedical Engineering*, vol. 65, no. 4, pp. 839–846, 2018.

[12] C. Leitão *et al.*, "Central arterial pulse waveform acquisition with a portable pen-like optical fiber sensor," *Blood Pressure Monitoring*, vol. 20, no. 1, pp. 43–46, 2015.

[13] C. Leitão *et al.*, "Plastic Optical Fiber Sensor for Noninvasive Arterial Pulse Waveform Monitoring," *IEEE Sensors Journal*, vol. 15, no. 1, pp. 14–18, 2015.

[14] J. Nedoma *et al.*, "Validation of a Novel Fiber-Optic Sensor System for Monitoring Cardio-respiratory Activities During MRI Examinations," *Advances in Electrical and Electronic Engineering*, vol. 15, no. 3, pp. 536–543, 2017.

[15] V. Budinski and D. Donlagic, "A Miniature Fabry Perot Sensor for Twist/Rotation, Strain and Temperature Measurements Based on a Four-Core Fiber," *Sensors*, vol. 19, no. 7, p. 1574, 2019.

[16] J. Zhu *et al.*, "An optical fiber Fabry–Perot pressure sensor using corrugated diaphragm and angle polished fiber," *Optical Fiber Technology*, vol. 34, pp. 42–46, 2017.
[17] F. Yu *et al.*, "Ultrasensitive Pressure Detection of Few-Layer MoS_2," *Advanced Materials*, vol. 29, no. 4, p. 1603266, 2017.
[18] C. Leitão *et al.*, "Optical fiber sensors for central arterial pressure monitoring," *Optical and Quantum Electronics*, vol. 48, no. 218, pp. 1–9, 2016.

Saroj Pullteap is, currently, an Associate Professor at Department of Mechanical Engineering, Silpakorn University. He received a Bachelor of Industrial Education in Computer Technology Program from King Mongkut's Institute of Technology North Bangkok in 2002, and also a Master of Engineering in Industrial Metrology from King Mongkut's University of Technology Thonburi in 2003. In 2007, he, consequently, received a Philosophy Doctor in Optical Engineering Program from the University of Toulouse, France. His research works are the development of a fiber optic sensor for mechatronics engineering and biomedical engineering applications.

Piyawat Samartkit received his Bachelor degree of Technology in Engineering Business from Silpakorn University, Thailand in 2018. He is continuing his study in Doctoral of Philosophy within the same university since 2018. His research interests include the development of fiber optic sensor for biomedical engineering applications and vital cardiovascular parameters monitoring.